A Concept for a High-Energy Gamma-ray Polarimeter

P. F. Bloser[a], S. D. Hunter[a], G. O. Depaola[b], and F. Longo[c]

[a]NASA Goddard Space Flight Center, Code 661, Greenbelt, MD 20771, USA

[b]Facultad de Matemática, Astronomía y Física, Universidad Nacional de Córdoba, Ciudad Universitaria, 5000 Córdoba, Argentina

[c]Department of Physics and INFN, via Valerio 2, I-34100 Trieste, Italy

ABSTRACT

We present a concept for an imaging gamma-ray polarimeter operating from ~ 50 MeV to ~ 1 GeV. Such an instrument would be valuable for the study of high-energy pulsars, active galactic nuclei, supernova remnants, and gamma-ray bursts. The concept makes use of pixelized gas micro-well detectors, under development at Goddard Space Flight Center, to record the electron-positron tracks from pair-production events in a large gas volume. Pixelized micro-well detectors have the potential to form large-volume 3-D track imagers with ~ 100 μm (rms) position resolution at moderate cost. The combination of high spatial resolution and a continuous low-density gas medium permits many thousands of measurements per radiation length, allowing the particle tracks to be imaged accurately before multiple scattering masks their original directions. The polarization of the incoming radiation may then be determined from the azimuthal distribution of the electron-positron pairs. We have performed Geant4 simulations of these processes to estimate the polarization sensitivity of a simple telescope geometry at 100 MeV.

Keywords: Polarimetry, Gamma-ray astronomy, pair production, gas detectors, Monte Carlo simulations

1. INTRODUCTION

Long recognized as a potentially valuable tool for high-energy astronomy, gamma-ray polarimetry is finally showing signs of becoming a viable observational technique. Traditional gamma-ray telescopes have thus far relied exclusively on imaging, spectroscopy, and timing to determine what physical processes are at work in high-energy sources. Due to low statistics, however, it is usually quite difficult to distinguish between competing physical models based on spectral and timing information alone. The promise of gamma-ray polarimetery stems from the fact that nearly all high-energy emission mechanisms can give rise to linearly polarized emission, though the polarization angle and degree of polarization are highly dependent on the source physics and geometry.[1] Both synchrotron radiation, produced by relativisitic electrons spiraling around magnetic field lines, and curvature radiation, caused by electrons following field lines that are themselves tightly curved, produce linearly polarized radiation in which the angle traces the field direction and the degree is independent of energy. Compton scattering of photons off electrons, on the other hand, produces scattered radiation whose polarization degree depends on energy and scatter angle. These processes are expected to dominate the high-energy radiation of gamma-ray pulsars, gamma-ray bursts (GRBs), supernova remnants (SNRs), active galactic nuclei (AGN), and X-ray binaries (XRB). An especially exciting possibility is the radiation produced by magnetic photon splitting, which may play a role in pulsars and soft gamma-ray repeaters with particularly strong magnetic fields. The two photons produced should have strong polarizations in which the angles depend on energy.[2] Thus gamma-ray polarization studies promise to provide a powerful new method for studying the physics of astronomical sources, just as polarization studies at optical and radio wavelengths have been doing for decades.

Despite this powerful scientific incentive, progress in the field of gamma-ray polarimetry has until recently been very slow. In principle, all three X-ray and gamma-ray interaction mechanisms – photoelectric absorption, Compton scattering, and pair production – are sensitive to the polarization vector of the incident photon: the

secondary products of the initial interaction – the photoelectron, Compton-scattered photon and recoil electron, or electron-positron pair, respectively – are produced with momenta described by a $\cos^2 \theta$ angular distribution relative to the incident electric field (whether the maximum lies parallel or perpendicular to the field depends on the process). High-energy polarimeters, therefore, depend on measuring the azimuthal distribution of the secondary particles. Until recent years, technological constraints have prevented the accurate measurement of this distribution, severely limiting the polarization sensitivity of gamma-ray telescopes. Chief amongst these constraints were the insufficient position resolution of the detectors, which restricts the accuracy to which the azimuthal angles can be determined, the small number of readout channels possible with practical electronics designs, which limits how finely a position-sensing detector may be segmented, and the effects of multiple Coulomb scattering of the secondary charged particles in detector materials, which quickly distorts their initial momentum vectors. Due to these factors, the two largest gamma-ray telescopes ever flown in space, COMTPEL and EGRET onboard the Compton Gamma-Ray Observatory (CGRO), had negligible polarization sensitivity.[1, 3, 4]

This situation is finally changing for polarimeters based on Compton scattering and photoelectric absorption. In the case of Compton telescopes, major advances in detector position resolution, event reconstruction algorithms, and high-density readout electronics have allowed new designs that are compact, permitting a large effective area, while maintaining good angular resolution and background rejection. The IBIS instrument on IN-TEGRAL will have some polarization sensivitiy for this reason,[5] and all currently discussed Advanced Compton Telescope (ACT) designs will naturally be highly sensitive to polarized radiation between several 100 keV and a few MeV.[6–10] Laboratory prototypes of dedicated Compton polarimeters have already demonstrated good sensitivity.[11, 12] Technological advances have also helped the cause of X-ray polarimetry using photoelectric absorption ($\sim$ 0.5–10 keV) through the emergence of micropattern gas detectors. These detectors combine a low-density gas medium with pixel readouts of very fine ($\sim 100~\mu$m) pitch, so that the initial track of the photoelectron may be accurately measured before it is distorted by Coulomb scattering. Good sensitivity has been demonstrated in the laboratory for X-ray polarimeters using this principle.[13, 14] Thus polarimetry at X-ray and medium energy gamma-ray energies seems nearly ready to become reality. The recent detection via the Compton scattering technique of very strong ($\sim 80\%$) linear polarization from the prompt emission of a GRB (0.15–2 MeV) by the RHESSI satellite[15] has moved gamma-ray polarization to the forefront of high-energy astrophysical investigations and provided a major spur to the development of future missions.

The flurry of activity in gamma-ray polarimetry has thus far not extended to the pair production regime ($\gtrsim 50$ MeV). This is despite the fact that it is in practice far easier to construct sensitive pair telescopes than Compton telescopes due to better angular resolution, simpler event reconstruction, and lower background. The same technological advances that have enabled the development of photoelectric X-ray polarimeters, namely very fine spatial resolution in a gas detector, should in principle minimize the Coulomb scattering of the electron-positron pair and thus finally also allow the construction of a pair telescope with polarization sensitivity. In this paper we describe a concept for a high-energy gamma-ray polarimeter based on gas micro-well detectors, amorphous silicon thin film transistor arrays, and high-density interconnect and readout electronics technology. This design is a natural extension of a next-generation high-energy gamma-ray telescope concept introduced previously.[16]

2. HIGH-ENERGY GAMMA-RAY POLARIMETRY

2.1. Basic Principles

The idea of measuring high-energy (> 50 MeV) gamma-ray polarization by detecting the asymmetric azimuthal distribution of the plane defined by the electron-positron pair has been discussed since the 1950s.[17] Much theoretical work has been done since then to calculate the polarization-dependent cross section and estimate the detrimental effects of multiple Coulomb scattering.[18–22] For the case where the incident photon, electron, and positron are nearly coplanar (i.e., the nuclear recoil is small), the azimuthal dependence of the cross section may be written[18]

$$\sigma(\psi) = \frac{\sigma_0}{2\pi}[1 + PR~\cos(2(\psi - \psi_0))], \tag{1}$$

where $\psi - \psi_0$ is the angle between the pair plane and the gamma ray's electric field vector, σ_0 is the total cross section, P is the fractional polarization, and $R \sim 0.1$ is a numerical factor expressing the inherent asymmetry

of the process. (More recent numerical calculations extend the cross section to non-coplanar pairs and suggest a more complex parameterization[22]; see Section 4.1.) In principle, then, one may search for polarized emission from a source by making a histogram of the recorded pair azimuth angles and fitting a function of the form $A \cos(2(\psi - \psi_0)) + B$. The strength of the azimuthal modulation may be expressed in terms of the modulation factor Q, usually defined as[1, 23]

$$Q = \frac{N_{max} - N_{min}}{N_{max} + N_{min}} = \frac{A}{B}, \tag{2}$$

where N_{max} and N_{min} are the number of counts recorded at the maximum and minimum of the distribution, respectively. In practice, rather than try to calculate R in Equation 1, one would determine the modulation Q_{100} resulting from 100% polarized radiation, either experimentally or by means of a Monte Carlo simulation. The degree of polarization measured from another source is then given simply by $P = Q_{measured}/Q_{100}$. More sophisticated statistical tests for the presence of azimuthal modulation have been developed as well[24]; the above basic formalism, however, yields a useful simple expression for the minimum detectable polarization (MDP) for a given instrument[23]:

$$MDP = \frac{n_\sigma}{Q_{100}S} \sqrt{\frac{2(S + B)}{T}}. \tag{3}$$

Here n_σ is the significance level, S is the source count rate in the detector, B is the background count rate, and T is the observation time. The polarization sensitivity can therefore be improved by increasing the effective area, decreasing the background, or increasing Q_{100}.

The effects of Coulomb scattering may be approximated by replacing the factor R in Equation 1 with

$$R' = R \, e^{-2\Phi^2}, \tag{4}$$

where $\Phi \sim 14L^{1/2}$ is the rms change in ψ (assuming a Gaussian distribution) due to multiple scattering after passing through L radiation lengths (RL) of material.[4, 20, 24] (Monte Carlo simulations have found this approximation for Φ to be overly pessimistic,[4, 24] but it is still useful for comparing different telescope designs.) Thus the scattering has the effect of exponentially lowering Q_{100}, or exponentially worsening the MDP. This is the primary reason why all pair telescopes to date, as well as those currently planned, have negligible polarization sensitivity. For example, the EGRET telescope allowed gamma rays to convert into pairs in tantalum conversion foils $L = 0.022$ RL thick. Although this gave the instrument a high efficiency, the resulting rms change in the pair azimuth in each foil was $\Phi = 2.1$ radians. Thus Q_{100} was reduced by a factor of 10^{-4}, making EGRET insensitive to polarization from even the strongest cosmic sources.[4, 24] Currently planned instruments such as AGILE and GLAST use the same detection method of thick conversion foils, meaning that they too will not have a useful sensitivity to polarization.

2.2. Advantages of a Gas Detector

The design of a polarimeter with, for example, sensitivity 10^3 times that of EGRET, i.e. with $R'/R = 10^{-1}$, requires, from Equation 4, that the direction of the electron and positron be determined after traversing a distance of $\sim 6 \times 10^{-3}$ RL. This distance, about one-fourth the thickness of one EGRET conversion foil, implies a track imaging detector with low density in terms of RL per sample measurement distance. A design for a next-generation high-energy gamma-ray telescope capable of arcminute single photon angular resolution requires a similar low-density track imager.[16] It was found that arcminute resolution is achievable only above ~ 3 GeV and requires a track imaging detector with density less than $\sim 2 \times 10^{-5}$ RL per sample. Using this design, the 6×10^{-3} RL would correspond to about 300 samples along the electron and positron tracks, more than sufficient to accurately determine the pair momenta. Such a low ratio of RL to sampling length can be achieved using gas detectors with very fine spatial resolution.

3. ADVANCED PAIR TELESCOPE AND HIGH-ENERGY POLARIMETER DESIGN

We have developed a concept for a high-energy gamma-ray telescope using gas micro-well detectors to achieve good polarization sensitivity. In this section we describe the detectors and readout electronics and present our concept for an advanced pair telescope (APT). The expected polarimetry performance is discussed in Section 4.
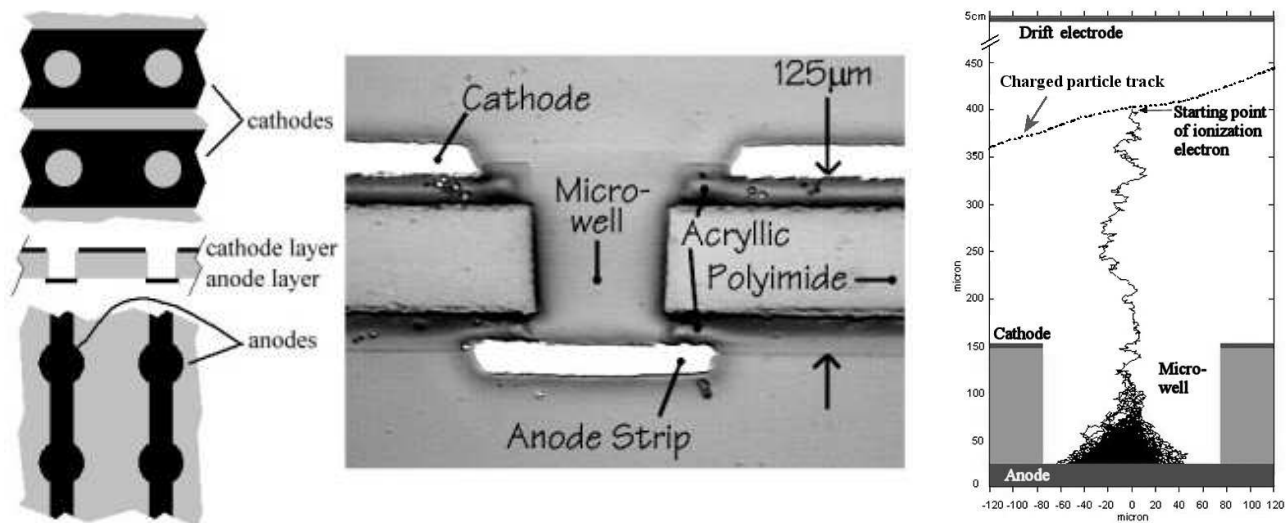
Figure 1. Micro-well detectors. *Left:* Copper cathode (top) and anode (bottom) traces for crossed-strip design. Wells are formed by exposing the anode through the cathode and substrate. *Center:* Cross section of an individual well formed by UV laser ablation with a polymide substrate.[25, 26] *Right:* Schematic of complete micro-well detector. The drift electrode defines the active region, in which fast charged particles generate ionization electrons which drift into the wells. Charge amplification takes place in the high-field avalanche region inside each well. The vertical scale has been greatly compressed.
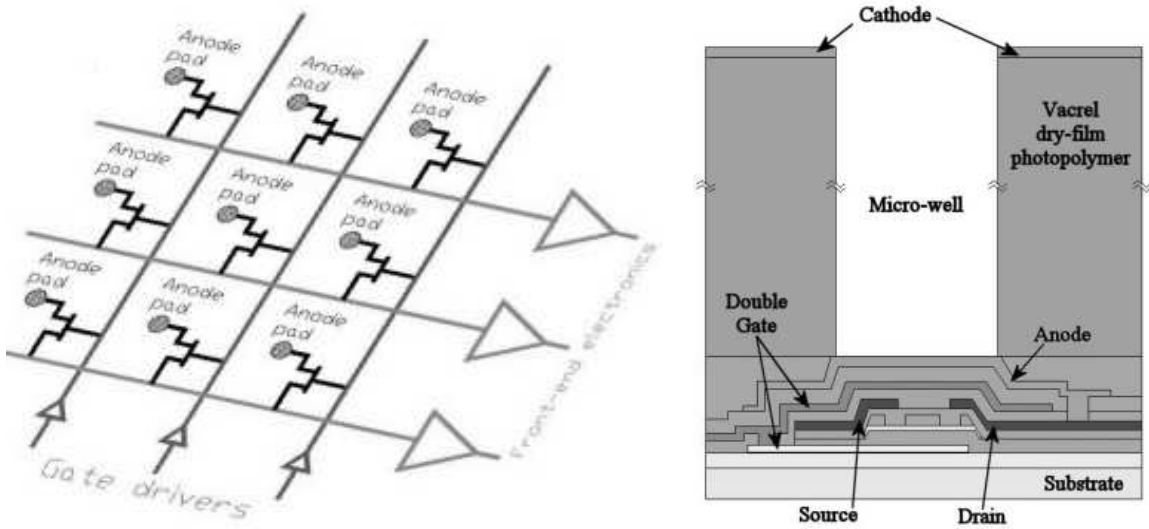
3.1. Pixelized Gas Micro-Well Detectors

The micro-well detector[25–27] is a type of gas proportional counter related to the gas electron multiplier.[28] Each sensing element consists of a charge-amplifying well, as shown in Figure 1. The cathode and anode electrodes are deposited on opposite sides of an insulating substrate. The well is formed as a cylindrical hole through the cathode and substrate, exposing the anode. An array of such wells forms a detector. The active tracking volume is bounded by a drift electrode on one side and the wells on the other. Ionization electrons produced by the passage of a high-energy charged particle drift toward the anodes and into the wells. An ionization avalanche occurs in each well, where there is an intense electric field set up by the voltage applied between the anode and cathode. The electrons from the avalanche are collected on the anode, while an equal but opposite image charge is measured on the cathode.

Micro-well detectors have many advantages over conventional multi-wire proportional counters. The anodes and cathodes are rigidly affixed to the substrate, which simplifies construction and allows very fine pitch without electrostatic distortions. The detectors are very rugged and low cost, and the high intrinsic gain reduces the power required for readout electronics. The gain and the drift velocity are independently adjustable, allowing high gain to be combined with slow drift; this permits the detectors to be operated as time projection chambers. These properties make it practical to read out large gas volumes with very good three-dimensional position resolution at reasonable cost.

Goddard Space Flight Center has been producing micro-well detectors for the past several years on rugged polymide substrates using UV laser ablation.[25, 26] These detectors have been constructed in a crossed-strip geometry, with the cathodes and anodes forming orthogonal strips on opposite side of the substrate, to allow simple two-dimensional imaging at X-ray energies. Very good detector performance has been observed,[25–27] including stable operation at gas gains of 3×10^4 in Ar- and Xe- based gases, the ability to sustain repeated breakdowns without damage, a FWHM energy resolution of 18% for 5.9 keV X-rays in 95% Xe/5% CO_2 gas, and a FWHM position resolution of ~ 200 μm for 400 μm well pitch.

The crossed-strip readout used for X-ray imaging is not ideal for recording extended tracks from charged particles. Thus we are currently focused on the development of pixelized micro-well detectors (PMWDs) together

Figure 2. The pixelized micro-well detector concept. *Left:* Readout of a pixelized detector using a TFT array. The gate drivers are activated sequentially, allowing each column to be read out in turn by the charge-integrating front end electronics. *Right:* Cross section of a single integrated a-Si:H TFT/micro-well detector pixel. The drift electrode is not shown. The vertical scale is exaggerated.

with collaborators at the Pennsylvania State University (Figure 2). The anodes are segmented into individual pixel pads, each of which is connected to an element of a thin-film transistor (TFT) array. The individual transistor gates are connected in columns, and the outputs are connected in rows. The gate drivers for each column are then activated sequentially, allowing the charge collected on the anode pads to be read out by charge-intergating amplifiers at the end of each row. Thus a two-dimensional projected image of the charged particle track is recorded. The third dimension may be determined by measuring the drift time of the ionization electrons (see Section 3.2).

Our collaborators at Penn State have developed a tri-layer fabrication process for hydrogenated amorphous silicon (a-Si:H) TFTs and integrated TFT circuits on polyamide substrates. TFT arrays based on a-Si:H were first developed as drivers for flat-panel displays, and more recently as readout devices for medical imagers.[29] The current TFT structure consists of a 500 Å thick amorphous silicon active layer and 3000 Å thick silicon nitride layers as the gate dielectric and passivation layers. The structure includes a double gate to reduce leakage current and prevent the FET from turning on due to the electic field of the micro-well avalanche. Good electical performance has been observed, with $I_{on}/I_{off} \sim 10^8$ and a low threshold voltage of 0.8–2.5 V. Current work is focused on producing the micro-well detector and TFT arrays as one integrated unit (Figure 2, right) using 100 μm thick-film photolithographic processing. The cathode and anodes are patterned on the film, and the wells are created by etching. Integrated PMWD-TFT detectors with a pitch of 200 μm are currently being produced for testing.

The small pitch and large area of PMWDs imply a very high density for the readout electronics and interconnects. The front-end charge-integrating preamplifiers, gate drivers, and time-projection electronics will all require ~ 50 channels cm^{-1} for the detectors described above. This requires an ASIC implentation for the electronics. Two charge-integrating amplifiers in an ASIC package currently under consideration for the PMWDs are the IDEAS VA-SCM2 chip and the Indigo ISC9717 chip. We are also investigating tape-carrier packaging and tape automated bonding as means to achieve our high-density interconnects in a compact, modular manner appropriate for a space-flight instrument.

3.2. Advanced Pair Telescope Concept

The APT imager concept is driven by the requirement to achieve a density of less than 2×10^{-5} RL per sample (Section 2.2). The PMWD-TFT array detectors described above with 200 μm well pitch (and corresponding drift
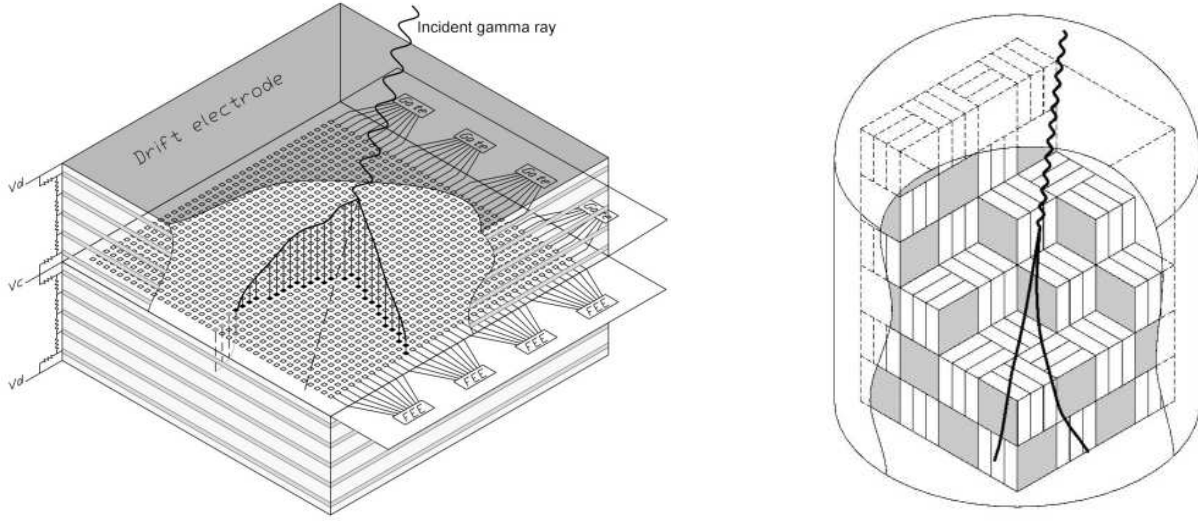
Figure 3. *Left:* The TTID is based on pixelized micro-well detectors. Each individual TTID consists of two back-to-back PMWD-TFT arrays (indicated by the array of squares), their front end electronics (FEE) and gate driver electronics (Gate), two drift electrodes (top and bottom), and four support walls. The walls are ringed with field shaping electrodes. The drift timing electronics (not shown) are located on the same circuit board as the gate driver electronics. *Right:* Instrument concept for the Advanced Pair Telescope. The APT instrument consists of a number of individual TTID modules, stacked and arranged in layers, with the entire stack enclosed in a pressure vessel. No calorimeter is required since the electron and positron energies may be measured via their multiple scattering.

distance resolution) and a xenon gas mixture at a pressure of $P \sim 1.5$ atmospheres (RL $\sim 15 \times (1 \text{ atm}/P)$ m), achieves this density requirement. These PMWD-TFT arrays would be packaged into three-dimensional track imaging detector (TTID) modules (Figure 3, left). The APT track imager concept (Figure 3, right) consists of a large number of TTID modules. Each module contains two back-to-back imagers bounded by drift electrodes and field shaping electrodes on the four walls. The front-end, gate driver, and drift timing electronics are distributed around the periphery of the module and folded and attached to the walls of the module.

Photons undergo pair production in the active gas volume of the TTID, defined by the TFT array and the drift electrode. The electron and positron traverse the gas leaving a trail of ionization that drifts into the array of micro-wells. The electron and positron also excite the xenon gas, producing UV scintillation light ($\lambda \sim 180$ nm) that provides a prompt start signal for the drift timing and, combined with the signals from an anticoincidence detector, the event trigger.

The low density necessarily requires a large gas depth to obtain a reasonable pair conversion probability and instrument effective area. For xenon at 1.5 atm, 0.5 RL (as in EGRET) corresponds to a depth of 5 m. We therefore envision a pair telescope consisting of stacked layers of TTID modules in the form of a cylinder 5 m deep and 2.5 m in diamter. Modules in successive layers are rotated by 90° so that the drift direction alternates, giving "stereo" projected images of the pair tracks. This give a redundant means of determining the three-dimensional paths of the tracks. Even though the gamma-ray incident direction and polarization angle are determined within about 6×10^{-3} RL ~ 6 cm of the vertex, the electron and positron continue to traverse the remainder of the gas. Since the entire depth of gas is instrumented, measuring the Coulomb scattering of the electron and positron can be used to determine their energy without the need for a massive calorimeter.[16] It may also be possible to use an outer layer of gas as an anticoincidence layer, removing the need for a massive plastic shield dome.
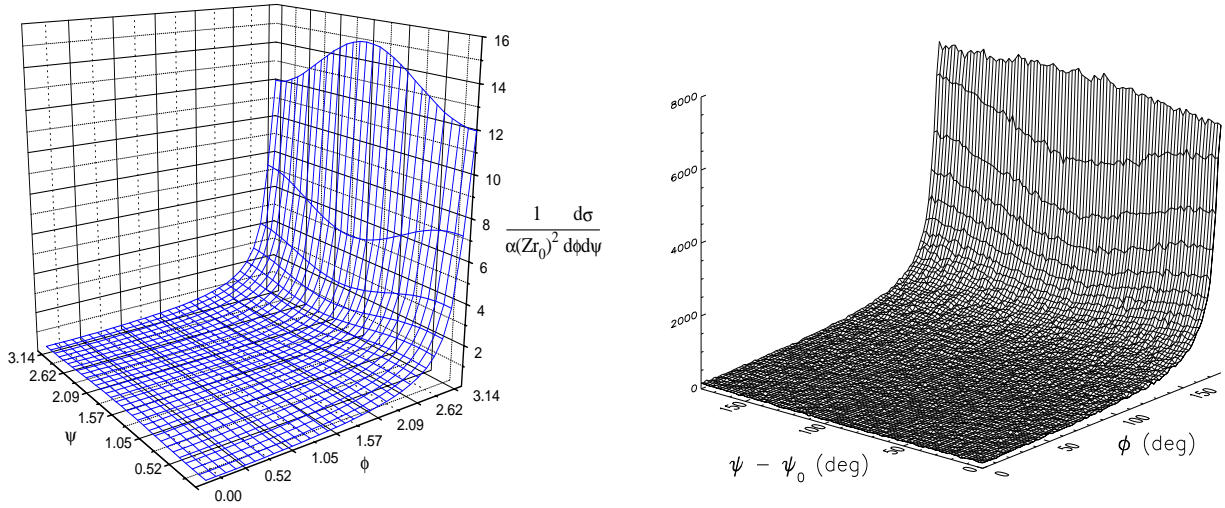
Figure 4. The shape of the polarized pair production cross section surface implemented in Geant4. *Left:* The cross section surface calculated by Depaola.[31]   Note that for $\phi \sim 180°$ the most likely ψ angle is perpendicular to the polarization vector (i.e., $\psi - \psi_0 = 90°$), whereas for even slightly non-coplanar events the most likely ψ is parallel to the polarization vector. *Right:* A simulation was performed using 5×10^6 events, and a two-dimensional histogram was made of the resulting ψ and ϕ angles with $2°$ bins to verify the form of the cross section. The results are in good agreement with the calculated cross section.

4. PREDICTED GAMMA-RAY POLARIMETER PERFORMANCE

Preliminary estimates of the polarization sensitivity of the APT concept described in Section 3.2 have been made using Geant4[30] Monte Carlo simulations. These results should be considered tentative, given the experimental nature of the Geant4 polarized pair production class. In addition, the simulations were performed using Geant4 version 5.0, which has recently been shown to produce electron-positron multiple scattering results with an rms scattering angle $\sim 20\%$ lower than that predicted by Molière theory. We therefore consider our results preliminary.

4.1. Geant4 Simulations of Polarized Pair Production

Polarized pair production has been implemented in Geant4 by G. Depaola and F. Longo.[22, 31, 32]   The cross section for the pair production process, including the polarization of the incident photon and the effects of non-coplanarity, has been derived analytically and calculated numerically. Integrating over the energies and polar angles of the pair, this yielded the cross section as a function of the azimuthal offset from the polarization vector $\psi - \psi_0$ and the non-coplanarity angle ϕ, defined as the angle between the electron and positron momenta projected into the plane normal to the incident photon (i.e., $\phi = 180°$ for coplanar events). This calculated cross section surface is shown in Figure 4 (left). An analytic parameterization of this surface is used for the Geant4 Monte Carlo sampling. Rather than the simple functional form of Equation 1, the parameterization takes the form $f(\phi, \psi) = f_{\pi/2}(\phi) \sin^2 \psi + f_0(\phi) \cos^2 \psi$, where $f_{\pi/2}(\phi)$ and $f_0(\phi)$ are functions of ϕ whose coefficients are themselves functions of energy. The parameterization agrees with the numerically calculated surface to within 5%. The cross section surface as implemented within Geant4 is shown in Figure 4 (right), recovered from a simultaion using 5×10^6 events. This surface is simply a two-dimensional histogram of the recorded ψ and ϕ angles (with $2°$ bins), ignoring the effects of multiple scattering. The results of the simulation (Figure 4 right) are in good agreement with the calculated cross section[22] (Figure 4 left), verifying that the Geant4 polarized pair production class is functioning as expected. Note that for very nearly coplanar events ($\phi \sim 180°$) the most likely ψ angle is perpendicular to the polarization vector (i.e., $\psi - \psi_0 = 90°$), but that for even slightly non-coplanar events the most likely ψ is parallel to the polarization vector, as pointed out by Depaola.[22]   In
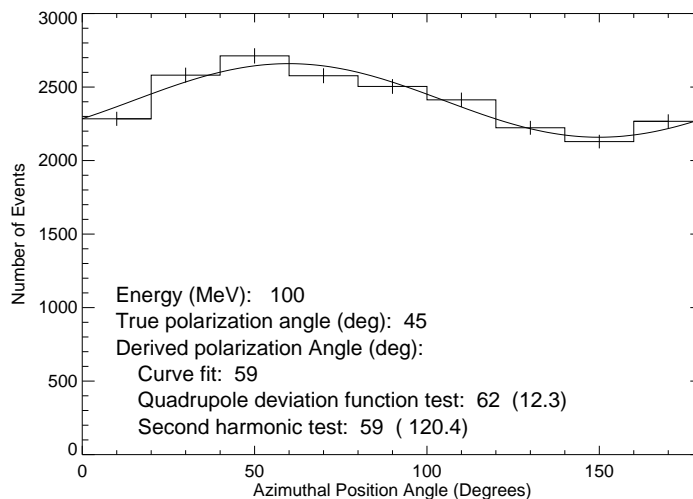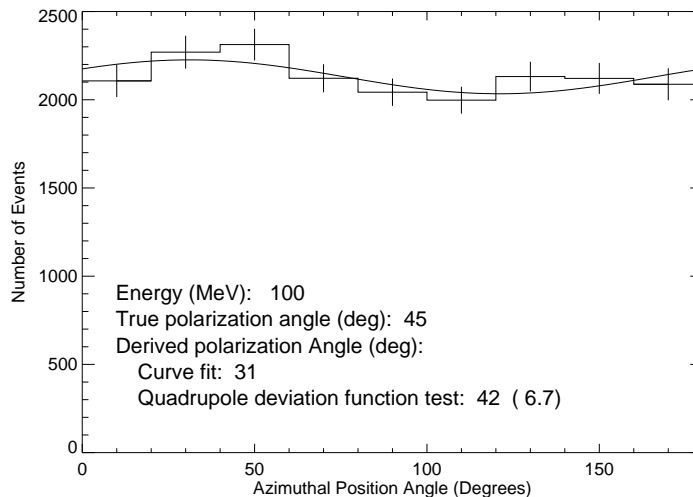
Figure 5. Output of the Geant4 polarized pair production process for 100 MeV photons in xenon gas. The effects of Coulomb scattering and detector binning are not included. The derived polarization angle found by curve fitting is $59°$, whereas the input angle was $45°$; the difference is due to the non-coplanar events. The modulation factor is $Q_{100} = 0.104$. The quadrupole deviation function and second harmonic tests also find an angle of $\sim 60°$; the values of the test statistics are given in parentheses.

practice a telescope would record the maximum at $\psi - \psi_0 = 0°$, since multiple scattering and imperfect position resolution would mask the azimuthal shape at $\phi \sim 180°$.

Simulations were performed for the simple case of 100 MeV gamma rays with a fixed polarization vector entering a xenon gas volume 5 m deep. No passive material was included in the mass model. During the tracking of the charged pair particles the step size was constrained to be 100 μm, or less than the pixel pitch, since otherwise energy was only deposited when a δ-ray with energy greater than 1 keV was generated. No detector response was included in the simulation; rather, the raw output (the exact positions of all energy deposits) was dumped into an output file, and the response of the detectors was applied in a separate program. This response included the effects of electron diffusion in the xenon gas,[33] binning into well pixels with a pitch of 200 μm, and the expected error in the drift distance, assumed to be equal to the position resolution of the detectors (taken to be one-half the well pitch, or 100 μm). Finally, a simple event reconstruction algorithm was applied: the two longest, straightest tracks were fit with a straight line for as long a distance as possible, and this was used to determine the infall direction and azimuth angle of the pair plane. A simple energy-weighting of the infall direction, according to the inverse of the rms scattering along each track, has been implemented, but this produced only a small improvement in the angular resolution.

Figure 5 shows the output of the Geant4 pair polarization process. Events were selected from the raw event file, taking the exact positions of all energy deposits and using only the first two hits of the electron and positron tracks (100 μm from the vertex) to define the initial pair momenta. Thus the effects of Coulomb scattering and detector binning were removed and only the effect of the parameterized cross section should be present. Only events falling within an angular radius containing 68% of all events were included. The input polarization angle was $45°$.

The presence of an azimuthal modulation was searched for in several ways. The first is a simple function fitting as described in Section 2.1. This yielded a polarization angle of $\psi_0 = 59°$ and a modulation factor $Q_{100} = 0.104$. The second method is the "quadrupole deviation function test" used to search COS B data for evidence of polarization from the Vela Pulsar.[24, 34] The test statistic must exceed 4.1 for a 3σ detection of azimuthal asymmetry. The test statistic for this dataset, given in parentheses in Figure 5, is 12.3, a very significant detection. The polarization angle is found to be $62°$ by this method. The third method is the even

2500

2000

1500

Number of Events

1000

500

0

Energy (MeV): 100
True polarization angle (deg): 45
Derived polarization Angle (deg):
  Curve fit: 31
  Quadrupole deviation function test: 42 (6.7)

0   50   100   150
Azimuthal Position Angle (Degrees)

Figure 6. Azimuthal distribution obtained from Geant4 after applying detector response and event reconstruction routines. Only event within the 68% angular radius are included, given a total of $\sim 1.9 \times 10^4$ events. The initial polarized distribution was divided by a normalized unpolarized distribution to remove systematics effects. The modulation factor is $Q_{100} = 0.045$.

more sensitive "second harmonic test" used to search for polarization signals in COS B and EGRET data.[4, 24] The value of the test statistic must exceed 13.8 for a 3σ detection. The test statistic for this dataset is 120.4, also a very significant detection. The polarization angle is found to be $59°$ for this test as well.

The shift in the polarization angle found by all three methods is the result of the non-coplanar events. The angle ψ used in the cross section is actually the azimuth angle of the momentum of the pair electron, projected into the plane perpendicular to the initial photon direction,[22] whereas a telescope can only measure the angle formed by the plane of the electron and positron. For $\phi \sim 180°$ these angles are nearly the same, and this is the case for which Equation 1 applies. For $\phi \lesssim 170°$, however, the angles are significantly different, and since a real telescope cannot recognize and exclude non-coplanar events, these events will systematically shift the azimuthal distribution recorded. In practice, since the shape of the cross section surface has been calculated as a function of energy, it should be possible to correct for this effect.

4.2. Expected Polarization Sensitivity

Out of 1.35×10^5 input events at 100 MeV, 3.0×10^4 produced pair events that were successfully reduced by the simple reconstruction algorithm, given an effective efficiency of $\sim 22\%$. (The reconstruction algorithm had trouble fitting events that included extended delta rays or very uneven energy splits between the electron and positron.) Only events within the 68% angular radius were included in the azimuthal histogram, as this would be the case for a real observation. This gave a total of $\sim 1.9 \times 10^4$ events. The 68% angular radius found using energy weighting of the pairs was $1.3°$. In order to recover the azimuthal distribution of the pairs it was necessary to repeat the simulation and reduction using unpolarized photons, and then to divide the polarized azimuth histogram by the normalized unpolarized histogram. The azimuthal distribution thus obtained is shown in Figure 6. Although the statistics are poor, a modulation similar to that in Figure 5 is evident. Due to the binning required to perform the division by the unpolarized histogram, it was not possible to apply the second harmonic test to this data (the second harmonic test operates on the individual azimuth values to increase sensitivity[24]). Both the curve fit and quadrupole deviation function tests find significant azimuthal asymmetry (the test statistic for the quadrupole deviation function test is 6.7), although they are unable to recover the input polarization angle from Figure 5. Better statistics should improve the determination of the polarization angle (this initial simulation was limited by time constraints). The modulation factor obtained from the curve fit is

$Q_{100} = 0.045$. Thus $R'/R \sim 0.45$, implying that the pair plane is indeed being measured within the 6×10^{-3} RL required from Section 2.2.

Using the results of the simulation, we may estimate the 3σ MDP from Equation 3. We assume a diameter of 2.5 m and a detection efficiency of 22%, giving an effective area of 10800 cm^2. Only events within a 68% angular radius of 1.3° are included. The background is taken to be events from the observed EGRET extragalactic diffuse background spectrum[35] which fall within the 68% angular radius. We consider a Crab-like source, and, for simplicity, assume a 100 MeV-wide energy band centered on 100 MeV. Then the 3σ MDP for a 1 Crab source is 40% in 10^6 s of observation time. In 10^7 s of observing time, or about one year of real time, the MDP is 13%. The MDP for a 100 mCrab source in 10^7 s is 41%. These numbers, while preliminary, indicate that this APT concept will have a useful polarization sensitivity for bright sources around 100 MeV.

5. CONCLUSIONS

Our preliminary Geant4 simulations of polarized pair production indicate that an APT consisting of PMWD-TFT gas detectors will be capable of detecting linearly polarized emission from bright sources at 100 MeV. There are several possible methods of improving the sensitivites derived in Section 4.2 that we will explore in more detailed simulations. These include limiting the effects of drift electron diffusion by shortening the drift distance, and improving the event reconstruction algorithms. Due to the inherent weakness of the azimuthal asymmetry for polarized pair production, however, the most effective means may be simply to increase the number of events available. Since the angular resolution of a gas pair telescope is exceptionally good, including events out to greater than the 68% angular radius used for EGRET should not increase the background too much. It may also be possible to increase the diameter of the telescope, especially if a plastic anticoincidence shield is not required. For example, a 3 m diameter and inclusion of 90% of the events would improve the 3σ MDP for a 1 Crab source to 29% in 10^6 s.

Another possible improvement is the inclusion of triplet pair production events. Pair production can occur in the field of an electron in the conversion material as well as in the field of the nucleus, and the recoil momentum imparted to the electron will be modulated around the polarization vector in the same manner as the pair plane.[36] This recoil electron may be tracked in a gas detector, and the azimuthal distribution will be far easier to determine than that of the pair planes. The cross section for this process is reduced by a factor of $1/Z$ compared to nuclear pair production, so that it only occurs $\sim$ 2% of the time in xenon. Sensitivity to this process may therefore require lighter gases. Triplet production is not yet implemented in Geant4.

We will continue to improve our Geant4 mass model, detector response, and event reconstruction algorithms in order to explore the polarization sensitivity of our APT concept more thoroughly. We also plan to construct a prototype, together with our Penn State collaborators, and to test it at a polarized gamma-ray beam in 2006.

ACKNOWLEDGMENTS

REFERENCES

1. F. Lei, A. J. Dean, and G. L. Hills, "Compton polarimetry in gamma-ray astronomy," *Space Sci. Rev.* **82**, pp. 309–388, 1997.
2. M. Baring, "Photon splitting limits to the hardness of emission in strongly magnetized soft gamma repeaters," *Astrophys. Jour.* **440**, pp. L69–L72, 1995.
3. F. Lei, G. L. Hills, A. J. Dean, and B. M. Swinyard, "Characteristics of COMPTEL as a polarimeter and its data analysis," *Astrophys. Jour. Supp. Ser.* **120**, pp. 695–698, 1996.
4. J. R. Mattox, "The sensitivity of EGRET to gamma-ray polarization," *Exp. Astron.* **2**, pp. 75–84, 1991.
5. J. B. Stephen, E. Caroli, R. C. da Silva, and L. Foschini, "Gamma-ray polarisation measurements with INTEGRAL/IBIS," in *Gamma 2001*, S. Ritz, N. Gehrels, and C. R. Shrader, eds., *AIP Conf. Proc.* **587**, pp. 816–820, 2001.

6. T. J. O'Neill, et al., "Tracking, imaging and polarimeter properties of the TIGRE instrument," *Astron. Astrophys. Supp. Ser.* **120**, pp. 661–664, 1996.

7. G. Kanbach, R. Andritschke, P. F. Bloser, F. Schopper, V. Schönfelder, and A. Zoglauer, "Concept study for the next generation medium-energy gamma-ray astronomy mission – MEGA," in *X-Ray and Gamma-RayTelescopes and Instruments for Astronomy*, J. E. Truemper and H. D. Tananbaum, eds., *Proc. SPIE* **4851**, pp. 1209–1220, 2003.

8. E. Aprile, A. Bolotnikov, D. Chen, R. Mukherjee, and F. Xu, "The polarization sensitivity of the liquid xenon imaging telescope," *Astrophys. Jour. Supp. Ser.* **92**, pp. 689–692, 1994.

9. S. E. Boggs, et al., "Upcoming balloon flight of the nuclear Compton telescope," in *X-Ray and Gamma-Ray Telescopes and Instruments for Astronomy*, J. E. Truemper and H. D. Tananbaum, eds., *Proc. SPIE* **4851**, pp. 1221–1227, 2003.

10. J. D. Jurfess and R. A. Kroeger, "Progress towards an advanced Compton telescope," in *Gamma 2001*, S. Ritz, N. Gehrels, and C. R. Shrader, eds., *AIP Conf. Proc.* **587**, pp. 867–876, 2001.

11. M. L. McConnell, J. R. Ledoux, J. R. Macri, and J. M. Ryan, "A hard X-ray polarimeter for gamma-ray bursts and solar flares," in *X-Ray and Gamma-Ray Telescopes and Instruments for Astronomy*, J. E. Truemper and H. D. Tananbaum, eds., *Proc. SPIE* **4851**, pp. 1382–1393, 2003.

12. R. A. Kroeger, W. N. Johnson, J. D. Kurfess, and B. F. Phlips, "Gamma-ray polarimetry using a position sensitive germanium detector," *Nucl. Inst. Meth. A* **436**, pp. 165–169, 1999.

13. E. Costa, P. Soffitta, R. Bellazzini, A. Brez, N. Lumb, and G. Spandre, "An efficient photoelectric X-ray polarimeter for the study of black holes and neutron stars," *Nature* **411**, pp. 662–665, 2001.

14. J. K. Black, P. Deines-Jones, S. E. Ready, and R. A. Street, "X-ray polarimetry with an active-matrix pixel proportional counter," *Nucl. Inst. Meth. A* , in press.

15. W. Coburn and S. E. Boggs, "Polarization of the prompt γ-ray emission from the γ-ray burst of 6 December 2002," *Nature* **423**, pp. 415–417, 2003.

16. S. D. Hunter, D. L. Bertsch, and P. Deines-Jones, "Design of a next generation high-energy gamma-ray telescope," in *Gamma 2001*, S. Ritz, N. Gehrels, and C. R. Shrader, eds., *AIP Conf. Proc.* **587**, pp. 848–852, 2001.

17. G. C. Wick, "Detection of gamma-ray polarization by pair production," *Phys. Rev.* **81**, pp. 467–468, 1951.

18. L. C. Maximon and H. Olsen, "Measurement of linear photon polarization by pair production," *Phys. Rev.* **126**, pp. 310–319, 1962.

19. S. R. Kel'ner, Y. D. Kotov, and V. M. Logunov, "Methods of measuring linear polarization of gamma quanta," *Sov. Jour. Nucl. Phys.* **21**, pp. 313–315, 1975.

20. A. A. Kozlenkov and I. G. Mitrofanov, "Polarimetry of cosmic sources of hard gamma-ray emission," *Sov. Astron.* **29**, pp. 591–593, 1985.

21. Y. D. Kotov, "Methods of measurement of gamma-ray polarization," *Space Sci. Rev.* **49**, pp. 185–195, 1988.

22. G. O. Depaola, C. N. Kozameh, and M. H. Tiglio, "A method to determine the polarization of high energy gamma rays," *Astropart. Phys.* **10**, pp. 175–183, 1999.

23. R. Novick, "Steller and solar X-ray polarimetry," *Space Sci. Rev.* **18**, pp. 389–408, 1975.

24. J. R. Mattox, H. A. Mayer-Hasselwander, and A. W. Strong, "Analysis of COS B data for evidence of linear polarization of Vela pulsar gamma rays," *Astrophys. Jour.* **363**, pp. 270–273, 1990.

25. J. K. Black, P. Deines-Jones, S. D. Hunter, and K. Jahoda, "Imaging micro-well detectors for X-ray and gamma-ray applications," in *X-ray and Gamma-ray Instrumentation for Astronomy XI*, K. A. Flanagan and O. H. W. Siegmund, eds., *Proc. SPIE* **4140**, pp. 313–323, 2000.

26. P. Deines-Jones, J. K. Black, H. Crawford, and S. D. Hunter, "Imaging micro-well proportional counters fabricated with masked UV laser ablation," *Nucl. Inst. Meth. A* **477**, pp. 55–58, 2002.

27. P. Deines-Jones, J. K. Black, S. D. Hunter, K. Jahoda, and S. M. Owens, "Large-area imaging micro-well detectors for high-energy astrophysics," *Nucl. Inst. Meth. A* **478**, pp. 130–134, 2002.

28. F. Sauli, "GEM: a new concept for electron amplification in gas detectors," *Nucl. Inst. Meth. A* **386**, pp. 531–534, 1997.

29. L. E. Antonuk, et al., "Large-area 97-mm pitch indirect-detection active-matrix flat-panel imager (AMFPI)," *Proc. SPIE* **3336**, pp. 2–13, 1998.

30. S. Agostinelli, et al., "Geant4 - a simulation toolkit," *Nucl. Inst. Meth. A* **506**, pp. 250–303, 2003.

31. G. O. Depaola and C. N. Kozameh, "Detecting polarized gamma rays by pair production," *Rad. Phys. Chem.* **53**, pp. 455–459, 1998.

32. G. O. Depaola, "Azimuthal distribution for pair production by high-energy γ-rays," *Nucl. Inst. Meth. A* **452**, pp. 298–305, 2000.

33. A. Peisert and F. Sauli, "Drift and diffusion of electrons in gases: a compilation," tech. rep. 84-08, CERN, 1984.

34. P. A. Caraveo, G. F. Bignami, I. Mitrofanov, and G. Vacanti, "Search for linear polarization in gamma-ray sources: possible evidence for the Vela pulsar," *Astrophys. Jour.* **327**, pp. 203–213, 1988.

35. D. A. Kniffen, et al., "EGRET observations of the high latitude diffuse radiation," *Astron. Astrophys. Supp. Ser.* **120**, pp. 615–617, 1996.

36. V. F. Boldyshev and Y. P. Peresun'ko, "Electron-positron pair photoproduction on electrons and analysis of proton beam polarization," *Sov. Journ. Nuc. Phys.* **14**, pp. 576–578, 1972.